Molecules MH_3 (M = Cr, Mo, W) Are Pyramidal: CCSD(T) Ab Initio Study of Structure and Vibrational Dynamics

Nikolai B. Balabanov and James E. Boggs*

Institute for Theoretical Chemistry, Department of Chemistry and Biochemistry, The University of Texas at Austin, Austin, Texas 78712

Received: March 22, 2000; In Final Form: June 6, 2000

Ab initio calculations were carried out on chromium, molybdenum, and tungsten trihydrides. The equilibrium parameters of the ground states, vibrational frequencies, IR intensities and the inversion barriers of the molecules were calculated at the CCSD(T) level with large basis sets. The relative energies to the excited states were evaluated by the EOM−CCSD method. All molecules were found to have pyramidal (C_{3v}) equilibrium structures. The calculated inversion barriers of CrH_3, MoH_3, and WH_3 are 1353, 1086, and 472 cm^{-1}, respectively. The vibrational levels corresponding to the totally symmetric H−M−H bending mode were predicted using the discrete variable representation approach. The tunneling splitting and rates were also evaluated within the Wentzel−Kramers−Brillouin approximation. The available experimental data are discussed in light of results from the ab initio calculations.

Introduction

In a previous paper[1] we reported the results of ab initio calculations of the equilibrium parameters, vibrational spectra, and vertical excited-state energies of some first-row transition metal trihydrides MH_3 (M = Sc, Ti, V, Fe). All of these molecules were found to have high spin ground electronic states and trigonal planar (D_{3h}) equilibrium structures. In this work we examine another group of the trihydrides: CrH_3, MoH_3, and WH_3.

The molecules CrH_3 and MoH_3 have been reported from spectroscopic studies[2,3] in inert gas matrices. In an experimental study of CrH and CrH_2 in which Cr vapor was co-condensed in an Ar matrix with atomic H or D, Van Zee et al.[2] found a band in the ESR spectrum that they thought might be attributable to CrH_3 in a quartet ground electronic state. Xiao et al.[3] later studied the UV-induced reaction of matrix-trapped Cr and Mo atoms with molecular H_2 and D_2 and reported spectral assignments for CrH_3 and MoH_3. Their results are discussed in detail below.

To our knowledge, there has been only one published result of ab initio calculations applied to the chromium family trihydrides. Based on Hartree−Fock−Slater (HFS) calculations, Ziegler[4] concluded that CrH_3 and MoH_3 prefer the trigonal planar geometry. However, it has been shown[1] that accuracy in determining the geometry of such molecules requires a good treatment of electron correlation, so we have undertaken a higher level theoretical study of these molecules.

Computational Details

Calculations were performed using a local version of the ACES II program package.[5] All-electron calculations were carried out for the CrH_3 molecule. A (14s11p6d1f/10s8p3d1f) basis set on Cr, and a (6s3p1d/4s2p1d) basis set on H were used. The Cr basis set was Wachters basis[6] modified as in the GAMESS[7] program and augmented with an *f*-function. The *f*-function exponent on the Cr atom was taken from ref 8. The H TZ2P basis set as implemented in ACES II is the (5s/3s) Dunning set[9] augmented with two optimized *p*-functions in (2,1) contractions of three primitives.[5] A diffuse *s*-function[10] and a polarization *d*-function[11] were also added to the TZ2P basis.

The averaged relativistic effective core potentials of Stevens et al.[12] were applied for metal atoms in calculations of MoH_3 and WH_3. The valence basis sets Mo(8s8p6d/4s4p3d) and W(7s7p6d/4s4p3d)[12] were augmented with 2*f* polarization functions. The Mo 2*f* set of Gaussian basis functions was obtained from a two-term fit to the optimal Slater exponent 2.33.[13] The tungsten *f* exponents were 0.8 and 0.3. Spherical *d* and *f* functions were used in all calculations.

Ground-state molecular parameters were computed at both unrestricted Hartree−Fock (UHF) and coupled cluster singles and doubles level augmented by perturbative correction for connected triple excitation (CCSD(T))[14,15] for all molecules. In the all-electron calculation equilibrium geometries were optimized using analytical gradients, and all vibrational frequencies and infrared intensities in the ground states were calculated using analytical second derivatives of the potential energy surface and analytical first derivatives of the dipole moment.[16] In the ECP calculations, equilibrium geometries, vibrational harmonic frequencies, and IR intensities were calculated numerically using the VIBMOL program.[17] Vertical excitation energies to other electronic states were evaluated with either the equation-of-motion coupled cluster method in singles and doubles approximation (EOM-CCSD)[18] or the quasi-restricted Hartree−Fock coupled cluster singles and doubles method (QRHF−CCSD).[19]

Because of tunneling between equivalent inversion conformations of these rather flat pyramidal structures, the vibration corresponding to their inversion mode cannot be treated as a simple harmonic oscillator. Their energy levels were computed by solving the appropriate one-dimensional Schroedinger equation

* To whom correspondence should be sent. FAX: 512-471-8696. E-mail: james.boggs@mail.utexas.edu.

10.1021/jp001087d CCC: $19.00
Published on Web 07/18/2000

$$\left\{\frac{1}{2\mu}\mathbf{P}^2(s) + \mathbf{V}(s)\right\}\Psi(s) = E\Psi(s) \quad (1)$$

using the discrete variable-finite basis representation (DVR/FBR) approach.[20] The nonrigid coordinate s corresponds to the height of the C_{3v} pyramidal structure (Figure 1), and the reduced mass $\mu = 3m_M m_H(m_M+3m_H)^{-1}$. The inversion potential $\mathbf{V}$ in eq 1 was represented by an even-power polynomial $\sum_{i=0}^{N} a_i s^{2i}$, which fits a numerical grid. The points on the grid were obtained by optimization of the energies of C_{3v} structures at several values of the angle γ between the M−H bond and the C_3 (z) symmetry axis of the molecule (Figure 1). The polynomial was of degree $N = 8$ for CrH_3 and MoH_3 and $N = 7$ for WH_3. In FBR/DVR calculations, the FBR basis $\phi_k(s)$ consisted of the eigenfunctions of the operator of the kinetic energy in eq 1

$$\phi_k(s) = \begin{cases} l^{-1/2} \sin\left(\frac{\pi k}{2l}s\right), & |s| < l \\ 0, & |s| > l \end{cases} \quad (2)$$

where the boundary value l was chosen as 4.0 au. The DVR basis consisted of 250 equally spaced points.

The tunneling splitting and tunneling rates were also evaluated within the Wentzel−Kramers−Brillouin approximation using the technique described in ref 21. In these calculations a correction for the variation of the reduced mass $\mu(\gamma) = \mu(1+3m_H \sin^2(\gamma\text{-}90°)/m_M)$ was taken into account.

Results and Discussion

A. Equilibrium Structures and Parameters. All of the molecules CrH_3, MoH_3, and WH_3 were found to have pyramidal (C_{3v}) equilibrium structures in their ground $^4A_2$ electronic states. All amplitudes in the CCSD wave functions of the MH_3 ground states were less than 0.1; therefore, the molecules can be satisfactorily treated with single-reference based correlation methods. The equilibrium metal−hydrogen distances at constrained planar (D_{3h}) and pyramidal conformations, valence H−M−H angles, dipole moments, and the inversion barriers of the molecules are given in Table 1; the harmonic wavenumbers and IR intensities are listed in Table 2.

Note that in contrast to the CCSD(T) calculations, the Hartree−Fock one predicts the CrH_3 pyramidal structure not to be a minimum on the potential energy surface of this molecule; the UHF calculations of vibration lead to an ω_4 imaginary harmonic frequency. The molecular parameters in MH_3 are very much influenced by electron correlation. The correlation effect is to shorten the M−H internuclear distances by amounts of 0.04−0.06 Å and to decrease the H−M−H valence angles by 2.4−3.0°. As expected, with shortening of the M−H bond lengths, the magnitudes of the stretching harmonic wavenumbers are increased relative to the UHF results. The electron correlation leads to strong decreases of the A_3 infrared intensities, which are the largest absorption in these molecules. The correlation effect on the inversion barriers in MH_3 has no systematic behavior. Accounting for electron correlation significantly decreases the inversion barrier in CrH_3, barely affects it in MoH_3, and increases it in WH_3.

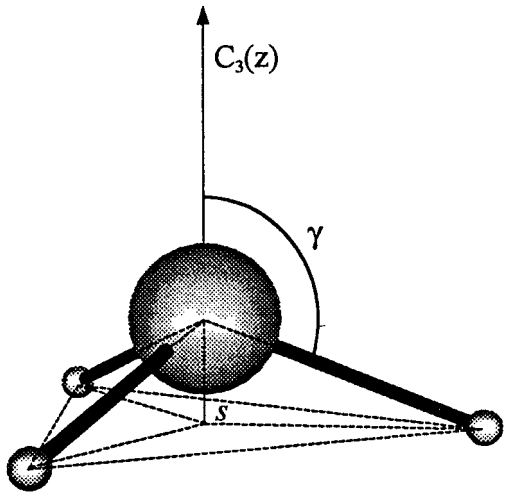

Figure 1. Notation of the inner coordinates in pyramidal MH_3 molecules.

In all of our molecules, the metal−hydrogen bond lengths shorten in the pyramidal structures compared to the planar trigonal one by 0.01 Å. The M−H distances increase sharply from CrH_3 to MoH_3 and then shorten slightly from MoH_3 to WH_3. Apparently, shortening of the W−H distance compared to the Mo−H one is due to the lanthanide-contraction effect.[22,23] The inversion barrier heights decrease smoothly from CrH_3 to WH_3, and one could expect that the H−M−H angles would increase in this series. However, the valence angle decreases from CrH_3 to MoH_3 and then increases from MoH_3 to WH_3. The explanation for the decrease of the inversion barrier in the row is simply a decrease in the second-order Jahn−Teller distortion[24,25] of the trigonal planar conformations.

Our results do not agree with the conclusion about planarity of CrH_3 and MoH_3 reached in previous theoretical work[4] based on HFS calculations. Even our UHF calculations showed that pyramidal structures of both CrH_3 and MoH_3 have lower energy than trigonal planar ones.[26] The more reliable CCSD(T) results confirm the nonplanarity.

The authors of a spectroscopic study[3] also preferred the trigonal planar structure instead of pyramidal for interpretation of their IR spectra of CrH_3 and MoH_3 due to absence of bands corresponding to the totally symmetric stretching vibration. Nevertheless, they noted that their data were inadequate for reaching a strict conclusion about the molecular structure of these trihydrides. Indeed, both planar (D_{3h}) and pyramidal (C_{3v}) MH_3 have two stretching vibrations: the totally symmetric

TABLE 1: M−H Distances, Valence Angles, Dipole Moments, and Inversion Barriers, *h*, of MH_3 (M = Cr, Mo, W)

molecule	R_e(M−H) at D_{3h}, Å	R_e(M−H), Å	α(H−M−H), deg[a]	μ_z, D	h, cm^{-1} [b,c]	method[d]
CrH_3	1.683	1.668	111.2	3.147	1758	UHF
	1.623	1.610	108.4	2.976	1353	CCSD(T)
MoH_3	1.752	1.742	110.4	2.941	1088	UHF
	1.710	1.698	107.4	2.741	1086	CCSD(T)
WH_3	1.741	1.737	115.2	1.676	390	UHF
	1.700	1.689	112.8	1.658	472	CCSD(T)

[a] $\gamma = 180° - \cos^{-1}(\sin(\alpha/2)\cos 30°)$. [b] 1 cm^{-1} = 2.85914 × 10^{-3} kcal/mol = 1.19627 × 10^{-2} kJ/mol. [c] Total UHF and CCSD(T) energies (a.u.) of pyramidal structures: −1044.935256, −1045.551604 (CrH_3); -68.998216, −69.450598 (MoH_3); −68.757108, −69.109677 (WH_3). [d] Basis sets are given in the text.

TABLE 2: Harmonic Vibrational Wavenumbers (cm^{-1}) at Planar (D_{3h}) and Pyramidal (C_{3v}) Configurations and IR Intensities (km/mol) of MH_3 (M = Cr, Mo, W)

molecule	structure	ω_1	ω_2	ω_3	ω_4	method
CrH_3	D_{3h}[a]	1643	798i	1640	992	UHF
		1795	558i	1796	962	CCSD(T)
	C_{3v}[b]	1727 (6)[c]	534 (365)	1695 (1135)	103.7i (753)	UHF
		1829 (26)	466 (296)	1796 (677)	610 (157)	CCSD(T)
MoH_3	D_{3h}	1785	473i	1756	755	UHF
		1797	393i	1804	837	CCSD(T)
	C_{3v}	1813 (56)	437 (326)	1768 (2004)	633 (491)	UHF
		1843 (43)	394 (243)	1809 (1561)	585 (832)	CCSD(T)
WH_3	D_{3h}	1966	383i	1908	782	UHF
		1988	328i	1945	859	CCSD(T)
	C_{3v}	1970 (47)	410 (222)	1914 (1206)	711 (180)	UHF
		2012 (26)	396 (163)	1985 (776)	719 (178)	CCSD(T)

[a] $\Gamma_{vib}=A'_1 + A''_2 + 2E'$. [b] $\Gamma_{vib} = 2A_1 + 2E$. [c] IR intensities in parentheses.

stretch ν_1 of A'_1 or A_1 type and the asymmetric one ν_3 of E′ or E type, respectively. The asymmetric degenerate ν_3 vibration is IR active for both pyramidal and planar molecules, and as a rule has the largest IR intensity in MH_3 molecules. The totally symmetric stretch is forbidden for planar molecules and active for pyramidal ones. Ideally, the IR spectrum of a pyramidal molecule is supposed to have two bands, which correspond to stretching vibrations, but according to our calculation of IR intensities (see Table 2) the totally symmetric stretch ν_1 in both CrH_3 and MoH_3 molecules has a very small IR intensity and would be difficult to detect in the IR spectra. Therefore the IR spectra[3] can also be interpreted as arising from pyramidal MH_3 molecules.

B. Excited States. The energies of vertical excitation to other electronic states in CrH_3, MoH_3, and WH_3 at their trigonal planar conformation are listed in Table 3. The energies of quartet electronic states were found by EOM−CCSD calculations with the ground $^4A'_2$ state wave function as a reference. The energies of doublet electronic state $(e'')^3$, $^2E''$ and $(a'_1)^2(a''_2)^1$, $^2A''_2$ were calculated by the QRHF−CCSD method. The wave function of the $^2E''$ state was constructed from the closed-shell RHF wave function for the corresponding negative MH_3^- ion, the wave function of the $^2A''_2$ state was obtained from the closed shell RHF wave function for the corresponding positive MH_3^+ ion. It should be noticed that the amplitudes in the $^2A''_2$ CCSD wave functions were of reasonably small magnitude, while the maximum amplitudes in the CCSD wave functions of the $^2E''$ states were 0.49 (CrH_3), 0.17 (MoH_3), and 0.20 (WH_3). This indicates that the $(e'')^3$, $^2E''$ state, especially in CrH_3, may be better described by the use of a multireference correlation method. The energies of other doublet electronic states listed in Table 3 were evaluated by the EOM-CCSD method using $(a'_1)^2(a''_2)^1$, $^2A''_2$ doublet electronic states as the reference. In all of these calculations, the metal−hydrogen distances were fixed to the values which had been optimized for the ground planar structures at the CCSD(T) level.

The first excited state in CrH_3 is the high spin quartet $(e'')^2(e')^1$, $^4E'$ electronic state. According to the Jahn−Teller theorem[27,28] the degenerate $^4E'$ electronic state is an intersection of the adiabatic potential of other electronic states $^4A_1$ and $^4B_2$, which correspond to molecular conformations of C_{2v} symmetry. We performed the full C_{2v} geometry optimizations of the $^4A_1$ and $^4B_2$ electronic states at the EOM−CCSD level; the results are given in Table 4. The Jahn−Teller distortion of the trigonal planar structure of the $^4E'$ state is large: 47.7° for H−Cr−H angles and 0.08 Å for Cr−H distances. The Jahn−Teller stabilization energy of the $^4E'$ electronic state is also large (5246 cm^{-1}), corresponding to nearly half of the vertical splitting between the $^4E'$ and $^4A'_2$ electronic states (10 333 cm^{-1}).

TABLE 3: Vertical Excitation Energies of MH_3 (M = Cr, Mo, W) at Their D_{3h} Conformations

MH_3	state	energy	method
CrH_3	$(1e'')^2(5a'_1)^1$, $^4A'_2$	0	CCSD[a]
	$(1e'')^2(4e')^1$, $^4E'$	10333	EOM-CCSD
	$(1e'')^1(5a'_1)^1(4e')^1$, $^4A''_2$	11360	EOM-CCSD
	$(1e'')^3$, $^2E''$	12146	QRHF−CCSD
	$(1e'')^1(5a'_1)^1(4e')^1$, $^4A''_1$	12738	EOM-CCSD
	$(1e'')^1(5a'_1)^1(4e')^1$, $^4E''$	13627	EOM-CCSD
	$(1e'')^1(5a'_1)^2$, $^2E''$	21350	EOM-CCSD
	$(5a'_1)^2(4e')^1$, $^2E'$	27580	EOM-CCSD
	$(1e'')^2(4e')^1$, $^4E'$	36566	EOM-CCSD
	$(1e'')^2(3a''_2)^1$, $^4A''_2$	39626	EOM-CCSD
	$(5a'_1)^2(3a''_2)^1$, $^2A''_2$	58961	QRHF−CCSD
MoH_3	$(1e'')^2(4a'_1)^1$, $^4A'_2$	0	CCSD[a]
	$(1e'')^3$, $^2E''$	10833	QRHF−CCSD
	$(1e'')^2(3e')^1$, $^4E'$	15303	EOM-CCSD
	$(1e'')^1(4a'_1)^2$, $^2E''$	15468	EOM-CCSD
	$(1e'')^1(4a'_1)^1(3e')^1$, $^4A''_2$	15661	EOM-CCSD
	$(1e'')^1(4a'_1)^1(3e')^1$, $^4A''_1$	17033	EOM-CCSD
	$(1e'')^1(4a'_1)^1(3e')^1$, $^4E''$	17160	EOM-CCSD
	$(4a'_1)^2(3e')^1$, $^2E'$	26579	EOM-CCSD
	$(1e'')^2(2a''_2)^1$, $^4A''_2$	34302	EOM-CCSD
	$(4a'_1)^2(2a''_2)^1$, $^2A''_2$	49690	QRHF−CCSD
WH_3	$(1e'')^2(3a'_1)^1$, $^4A'_2$	0	CCSD[a]
	$(1e'')^1(3a'_1)^2$, $^2E''$	13045	EOM-CCSD
	$(1e'')^1(3a'_1)^1(3e')^1$, $^4A''_2$	13793	EOM-CCSD
	$(1e'')^3$, $^2E''$	13810	QRHF−CCSD
	$(1e'')^1(3a'_1)^1(3e')^1$, $^4A''_1$	14808	EOM-CCSD
	$(1e'')^1(3a'_1)^1(3e')^1$, $^4E''$	15108	EOM-CCSD
	$(1e'')^2(3e')^1$, $^4E'$	17066	EOM-CCSD
	$(3a'_1)^2(3e')^1$, $^2E'$	21797	EOM-CCSD
	$(1e'')^2(2a''_2)^1$, $^4A''_2$	32101	EOM-CCSD
	$(3a'_1)^2(4a'_1)^1$, $^2A'_2$	41774	EOM-CCSD
	$(3a'_1)^2(2a''_2)^1$, $^2A''_2$	41909	QRHF−CCSD

[a] CCSD total energies (a.u.) of $^4A'_2$ states: −1045.533651 (CrH_3), −69.429967 (MoH_3), −69.096782 (WH_3).

Nevertheless, the $^4A'_2$ electronic state remains the ground electronic state in CrH_3, even with the large Jahn−Teller effect in the lowest degenerate excited electronic state. The same conclusion will very likely also be valid for MoH_3 and WH_3. The lowest electronic states in MoH_3 and WH_3 at their trigonal planar conformations are the doublet $^2E''$ states. The $^2E''$ electronic states are also subject to Jahn−Teller distortion, which can lower their energies. But judging from calculations of Jahn−Teller stabilizations energies of the E″ electronic states in TiH_3 and VH_3[1] we expect the Jahn−Teller stabilization energies in the E″ states in MH_3 (M = Cr, Mo, W) to be small.

The only possible reason for the instability of the trigonal planar conformations of the MH_3 molecules in their quartet ground electronic states is a strong vibronic coupling of the ground state with appropriate excited electronic states.[25] The planar configuration has A'_2 symmetry and the inner coordinate

TABLE 4: C_{2v} Symmetry Equilibrium Geometries and Jahn−Teller Stabilization Energies of CrH_3 in First Excited Electronic State

	$^4A_1$	$^4B_2$
$R_1(Cr-H_{(1)})$, Å	1.733	1.563
$R_2(Cr-H_{(2)}) = R_3(Cr-H_{(3)})$, Å	1.592	1.681
$\alpha(H_{(2)}-Cr-H_{(3)})$, deg	83.8	167.7
ΔE_{JT}, cm^{-1}	4773	5246

TABLE 5: CCSD(T) Inversion Potentials of MH_3 (M = Cr, Mo, W)

molecule	γ, deg	V^{opt}, cm^{-1}	R^{opt}(M−H), Å	μ_z^{opt}, D
CrH_3	90	0.00	1.6235	0.0000
	95	−231.78	1.6229	0.8125
	100	−712.75	1.6201	1.5586
	105	−1151.23	1.6156	2.2554
	110	−1351.36	1.6101	2.9121
	115	−1197.44	1.6040	3.5290
	120	−629.96	1.5976	4.0994
	125	374.42	1.5910	4.6098
	130	1806.73	1.5847	5.0393
MoH_3	90	0.00	1.7097	0.0000
	95	−142.66	1.7086	0.6670
	100	−491.38	1.7059	1.3173
	105	−863.00	1.7024	1.9477
	110	−1073.40	1.6990	2.5647
	115	−1008.99	1.6956	3.1722
	120	−656.06	1.6917	3.7608
	125	−95.69	1.6858	4.3030
	130	547.49	1.6772	4.7502
WH_3	90	0.00	1.7001	0.0000
	95	−97.66	1.6986	0.5407
	100	−314.84	1.6948	1.0644
	105	−467.43	1.6898	1.5692
	110	−355.22	1.6848	2.0702
	115	164.40	1.6804	2.5911
	120	1134.60	1.6763	3.1558
	125	2482.36	1.6713	3.7756

TABLE 6: First Several Vibrational Levels, Which Correspond to Inversion Mode of MH_3 (M = Cr, Mo, W), Calculated by the DVR/FBR Method

V	CrH_3	MoH_3	WH_3
0	−1125.0[b]	−892.9[b]	−281.3
1	−1125.0	−892.9	−273.8
2	−684.3	−523.9	6.6
3	−682.6	−522.6	111.4
4	−282.9	−202.3	325.1
5	−257.0	−181.7	545.0
6	34.4	43.7	792.8
7	145.6	145.5	1058.4
8	321.3	323.0	1339.6
9	442.9	490.1	1634.3

[a] The zero of energy corresponds to the energy of the D_{3h} molecular conformation [b] Splittings between the first two levels in CrH_3 and MoH_3 are given in Table 7.

Q, which corresponds to the displacement of nuclei leading to the $D_{3h} \rightarrow C_{3v}$ deformation of the molecular structure, is of A''_2 symmetry, so the excited electronic states with which interaction leads to the instability of the planar conformations should have A''_1 symmetry. The first A''_1 electronic states in these molecules lie 12000 to17000 cm^{-1} higher than the ground state.

C. Vibrational Frequencies. The inversion potentials of the molecules calculated at the CCSD(T) level are given in Table 5. The energy levels which correspond to the inversion mode of the molecules are listed in Table 6. The inversion potentials and corresponding vibrational levels of H−M−H bending ν_2 (A_1) mode of CrH_3 and WH_3 are shown in Figure 2 and Figure 3, respectively; the inversion potential and the location of vibrational levels of MoH_3 are very similar to those of CrH_3.

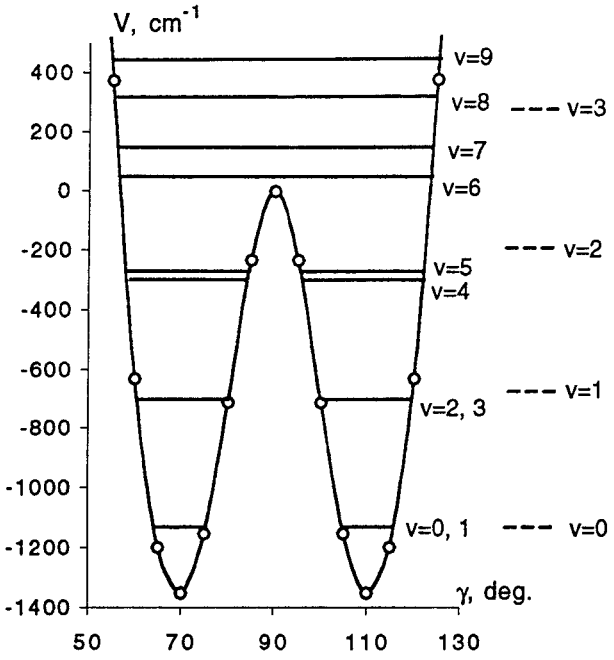

Figure 2. CrH_3 inversion potential and corresponding vibrational levels.

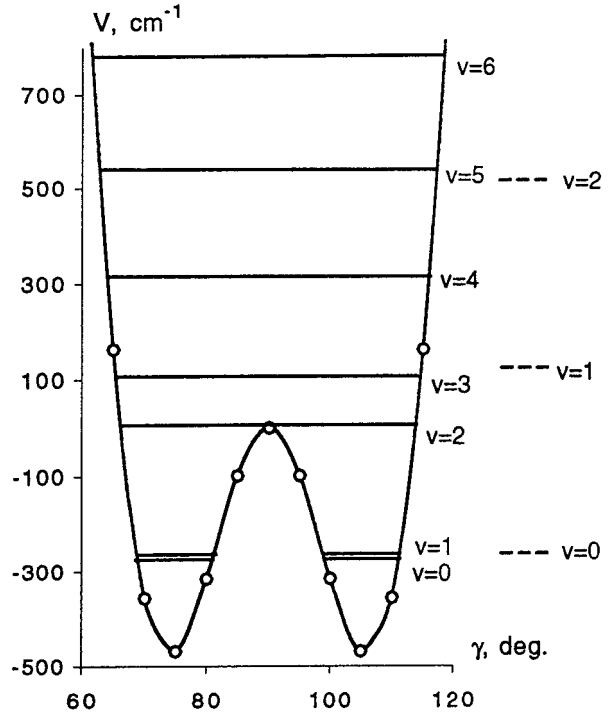

Figure 3. WH_3 inversion potential and corresponding vibrational levels.

The vibrational levels obtained from the harmonic approximation are also shown by dashed lines for comparison.

The tunneling splittings of the first two vibronic levels in CrH_3 and MoH_3 (Table 7) obtained with the DVR/FBR method have magnitudes which are less than the calculation error of finding vibronic energy levels with this method. Therefore we calculated the tunneling splittings by the WKB method, which is considered to be more accurate for tunneling splitting of small magnitudes.[21] Nevertheless, the DVR/FBR splitting frequencies are quite close to the WKB frequencies. Tunneling splittings of such magnitude can be measured by ultrahigh-resolution spectroscopy methods.

Only values of the ν_3 fundamental wavenumbers of CrH_3 and MoH_3 have been reported from experiment.[3] When comparing

TABLE 7: Tunneling Frequencies ν_T (cm^{-1}) and Tunneling Rates τ_T (s) for the ν_2 (A_1) Bending Mode

molecule	splitting	ν_T	τ_T	method
CrH_3	$0 \rightarrow 1$	0.0457	0.3648×10^{-9}	DVR/FBR
		0.0620	0.2690×10^{-9}	WKB
	$2 \rightarrow 3$	1.6976	0.9825×10^{-11}	DVR/FBR
		2.5451	0.6553×10^{-11}	WKB
MoH_3	$0 \rightarrow 1$	0.0317	0.5256×10^{-9}	DVR/FBR
		0.0225	0.7402×10^{-9}	WKB
	$2 \rightarrow 3$	1.3050	0.2781×10^{-10}	DVR/FBR
		0.8609	0.1937×10^{-10}	WKB

TABLE 8: Comparison of Scaled[a] Theoretical and Experimental[3] Wavenumbers of CrH_3 and MoH_3

molecule	ν_3, cm^{-1}	method
CrH_3	1706.2	theor.
	1513.0 }	IR(Ar)
	1509.0 }	
	1510.5 }	IR(Kr)
	1506.9 }	
MoH_3	1718.6	theor.
	1680.0	IR(Kr)
MoD_3	1224.2	theor.
	1202.0	IR(Kr)

[a] The theoretical harmonic wavenumbers were scaled by a factor 0.95 to take into account the error of theoretical approximation (see text).

the experimental and theoretical frequencies, one should take into account two sources of possible discrepancy. The first source is the error in the theoretical approximation, which includes the incompleteness of the basis sets, the neglect of correlation effects of still higher order, use of the effective core potential, and neglect of anharmonicity of the vibration in MH_3 molecules. We expect the error of the theoretical computation of fundamental transitions to be ~5%. Another source is that the MH_3 molecules were trapped in a matrix of Ar or Kr atoms during the spectroscopic experiment. The influence of the matrix on the structure and spectra of molecules usually leads to a decrease in the magnitudes of stretching wavenumbers relative to wavenumbers of free molecule, and sometimes to splitting of bands in the IR spectra.

A comparison of the theoretical and experimental[3] ν_3 wavenumbers is given in Table 8. For CrH_3 the theoretical ν_3 wavenumber is ~200 cm^{-1} higher than experimental. This discrepancy cannot be explained by anharmonicity or matrix effects. The authors reported[3] that in the reaction $Cr+H_2$ the peaks due to CrH_3 were much stronger than those assigned to MoH_3 in the reaction of Mo with H_2. This fact is also in conflict with our result; the ab initio IR intensity of the ν_3 vibration in CrH_3 is much less than that in MoH_3 (Table 2). This supports the suggestion of Ma et al.[29] that the observed band at 1510 cm^{-1} actually belongs to $CrH_2 \cdot H_2$, not CrH_3.

Our scaled ν_3 wavenumbers for MoH_3 and isotopic MoD_3 are in good agreement with values found in the IR study.[3] To predict the location of the band which corresponds to the totally symmetric ν_1 vibration of Kr-isolated MoH_3, we scaled the ab initio force field against the observed wavenumber $\nu_3 = 1680.0$ cm^{-1} using a standard scaling procedure.[30] We obtained the scaling coefficient for the M−H bond-stretching coordinate to be 0.862. Calculated with the scaled force field, $\nu_3 = 1711.5$ cm^{-1}.

Acknowledgment. This work was supported by a grant from the Robert A. Welch Foundation. We thank John Stanton for many interesting discussions and Hiroyasu Koizumi for help with the DVR/FBR calculations.

References and Notes

(1) Balabanov, N. B.; Boggs, J. E. *J. Phys. Chem. A* **2000**, *104*, 1597.
(2) Van Zee, R. J.; DeVore, T. C.; Weltner, Jr., W. *J. Chem. Phys.* **1979**, *71*, 2051.
(3) Xiao, Z. L.; Hauge, R. H.; Margrave, J. L. *J. Phys. Chem.* **1992**, *96*, 636.
(4) Ziegler, T. *J. Am. Chem. Soc.* **1983**, *105*, 7543.
(5) Stanton, J. F.; Gauss, J.; Watts, J. D.; Lauderdale, W. J.; Bartlett, R. J. *Int. J. Quantum Chem. Symp.* **1992**, *26*, 879.
(6) Wachters, A. J. H. *J. Chem. Phys.* **1970**, *52*, 1033.
(7) Schmidt, M. W.; Baldridge, K. K.; Boatz, J. A.; Elbert, S. T.; Gordon, M. S.; Jensen, J. H.; Koseki, S.; Matsunaga, N.; Nguyen, K. A.; Su, S. J.; Windus, T. L.; Dupuis, M.; Mongomery, J. A. *J. Comput. Chem.* **1993**, *14*, 1347.
(8) Botch, B. H.; Dunning, T. H.; Harrison, J. F. *J. Chem. Phys.* **1981**, *75*, 3466.
(9) Dunning, T. H. *J. Chem. Phys.* **1971**, *55*, 716.
(10) Dunning, T. H.; Hay, P. J. In *Methods of electronic structure theory*; Schaefer, H. F., III, Ed.; Plenum Press: New York, 1977; Vol. 2. This exponent was obtained from the Extensible Computational Chemistry Environment Basis Set Database, Version 1.0, as developed and distributed by the Molecular Science Computing Facility, Environmental and Molecular Sciences Laboratory which is part of the Pacific Northwest Laboratory, P.O. Box 999, Richland, WA 99352, USA, and funded by the U.S. Department of Energy. The Pacific Northwest Laboratory is a multiprogram laboratory operated by Battelle Memorial Institute for the U.S. Department of Energy under contract DE-AC06−76RLO 1830. Contact David Feller or Karen Schuchardt for further information.
(11) Frisch, M. J.; Pople, J. A.; Binkley. J. S. *J. Chem. Phys.* **1984**, *80*, 3265.
(12) Stevens, W. J.; Krauss, M.; Basch, H.; Jasien, P. G. *Can. J. Chem.* **1992**, *70*, 612.
(13) Walch, S. P.; Bauschlicher, C. W.; Nelin, C. J. *J. Chem. Phys.* **1983**, *79*, 3600.
(14) Raghavachari, K.; Trucks, G. W.; Pople, J. A., Head-Gordon, M. *Chem. Phys. Lett.* **1989**, *157*, 479.
(15) Bartlett, R. J.; Watts, J. D.; Kucharski, S. A.; Noga, J. *Chem. Phys. Lett.* **1990**, *165*, 513.
(16) Gauss, J.; Stanton, J. F. *Chem. Phys. Lett.* **1997**, *276*, 70.
(17) Solomonik, V. G., Doctor in Chemistry Thesis, Moscow State University, 1993.
(18) Stanton, J. F.; Bartlett, R. J. *J. Chem. Phys.* **1993**, *98*, 7029 and references therein.
(19) Rittby, M.; Bartlett, R. J. *J. Phys. Chem.* **1988**, *92*, 3033.
(20) Light, J. C.; Hamilton, I. P.; Lill, J. V. *J. Chem. Phys.* **1985**, *82*, 1400.
(21) Schwerdtfeger, P.; Laakkonen, L. J.; Pyykko, P. *J. Chem. Phys.* **1992**, *96*, 6807.
(22) Pyykko, P. *Chem. Rev.* **1988**, *88*, 563.
(23) Kaltsoyannis, N. *J. Chem. Soc., Dalton Trans.* **1997**, 1.
(24) Burdett, J. K. *Chem. Soc. Rev.* **1978**, 507.
(25) Bersuker, I. B.; Gorinchoi, N. N.; Polinger, V. Z. *Theor. Chim. Acta (Berl.)* **1984**, *66*, 161.
(26) A reviewer of this paper, Cory C. Pye, performed density function theory calculations on CrH_3 using the Gaussian 92 program and Ahlrichs TZV basis set obtained from EMSL online basis set library (ref 10). The best results were obtained using the B3LYP functional:

	R(Cr−H), Å	α(H−Cr−H), deg	E (a.u.)	freq, (cm^{-1})			
D_{3h}	1.6364	120.00	−1046.1636715	1666	528i	1682	709
C_{3v}	1.6178	107.00	−1046.1700019	1665	493	1691	612

Dr. Pye also contacted the author of ref 4 who pointed out that his calculations were done before gradient optimization techniques were available in the program used so that an incorrect structure was predicted due to the partial energy-only optimization.
(27) Englman, R. *The Jahn−Teller effect*, Wiley: New York, 1972.
(28) Bersuker, I. B.; Polinger, V. Z. *Vibronic Interaction in Molecules and Crystals*; Springer-Verlag: New York, 1989.
(29) Ma, B.; Collins, C. L.; Schaefer, H. F. *J. Am. Chem. Soc.* **1996**, *118*, 870.
(30) Fogarasi, G.; Pulay, P. In *Vibrational Spectra and Structure*; Elsevier: Amsterdam, 1985; vol. 14, pp 125−129.